Fractional Calculus and Applied Analysis (2023) 26:599–618
https://doi.org/10.1007/s13540-023-00138-3

ORIGINAL PAPER

General one-dimensional model of the time-fractional diffusion-wave equation in various geometries

Ján Terpák[1]

Received: 9 August 2022 / Revised: 17 February 2023 / Accepted: 20 February 2023 /
Published online: 20 March 2023

Abstract
This paper deals with the analysis of the time-fractional diffusion-wave equation as one-dimensional problem in a large plane wall, long cylinder, and sphere. The result of the analysis is the proposal of one general mathematical model that describes various geometries and different processes. Finite difference method for solving the time-fractional diffusion-wave equation using Grünwald-Letnikov definition for homogeneous or inhomogeneous material and for homogeneous or inhomogeneous boundary conditions is described. Dirichlet, Neumann and Robin boundary conditions are considered. Implementation of numerical methods for explicit, implicit, and Crank-Nicolson scheme were realised in MATLAB. Finally, illustrative examples of simulations using the developed toolbox are presented.

Keywords Fractional calculus (primary) · Time-fractional diffusion-wave equation · Finite difference method · Grünwald-Letnikov derivative · MATLAB toolbox

Mathematics Subject Classification 26A33 (primary) · 35R11 · 80M20

1 Introduction

The fundamental phenomena, such as diffusion and wave propagation, are described by the following partial differential equations [4], i.e.

– diffusion equation:

$$\frac{\partial u(\mathbf{r},t)}{\partial t} = D\nabla^2 u(\mathbf{r},t),$$

✉ Ján Terpák
jan.terpak@tuke.sk

[1] Institute of Control and Informatization of Production Processes, Technical University of Kosice, Nemcovej 3, 04200 Kosice, Slovakia

– wave equation:

$$\frac{\partial^2 u(\mathbf{r},t)}{\partial t^2} = c^2 \nabla^2 u(\mathbf{r},t).$$

Generalising the above partial differential equations by replacing the integer-order time derivatives with derivatives of fractional order $\alpha \in (0;2]$ the following time-fractional diffusion-wave equation is obtained:

$$\frac{\partial^\alpha u(\mathbf{r},t)}{\partial t^\alpha} = k^2 \nabla^2 u(\mathbf{r},t).$$

The standard (integer-order) diffusion or wave equation used for the description of many materials such as visco-elastic materials, granular and porous materials, composite materials, etc., is often not sufficiently adequate. In such cases, the description requires the development of more suitable models using fractional-order derivatives [13, 22, 28, 29, 44]. The causes are mainly roughness or porosity of the material [21–23], fractality and chaotic behavior of systems [3, 16, 24, 42], and memory of the systems and ongoing processes [25, 26, 35, 36, 41].

The time-fractional diffusion-wave equation as an adequate model requires the creation of new methods and tools for its solution. This topic is currently relevant and many important authors have contributed to its development, such as Fourier, Abel, Leibniz, Grünwald, Letnikov, Liouville, and Riemann [18, 22, 34].

Nowadays there is a number of numerical methods for solution of time-fractional diffusion-wave equation. These methods are based on the finite difference method (FDM) [37, 39, 46], the finite element method [5, 6, 33], the random walk models [8, 14, 15], Monte Carlo simulation [7, 17, 30], the method of Adomian decomposition [10, 19], numerical quadrature [2, 12, 43], and matrix approach [9, 27–29]. FDM is an extended method, where explicit, implicit and Crank-Nicolson schemes are used [44]. In the case of different geometries, we know the solutions for a planar wall, a cylinder and a sphere [1, 11, 20, 31, 32, 38, 45], but for the general geometry this is not reported yet.

Therefore, the present work aims at the design, numerical solution and MATLAB implementation of the general one-dimensional model of the time-fractional diffusion-wave equation applied to the time-fractional heat conduction problem in various geometries. This is presented in Fig. 1, which can be considered as an outline and a graphical abstract.

2 Time-fractional heat conduction models

The one-dimensional time-fractional heat conduction model in different geometries can be expressed as follows:

– in a large plane wall

$$\varrho c_p \frac{\partial^\alpha T(r,t)}{\partial t^\alpha} = \frac{\partial}{\partial r}\left(\lambda \frac{\partial T(r,t)}{\partial r}\right),$$

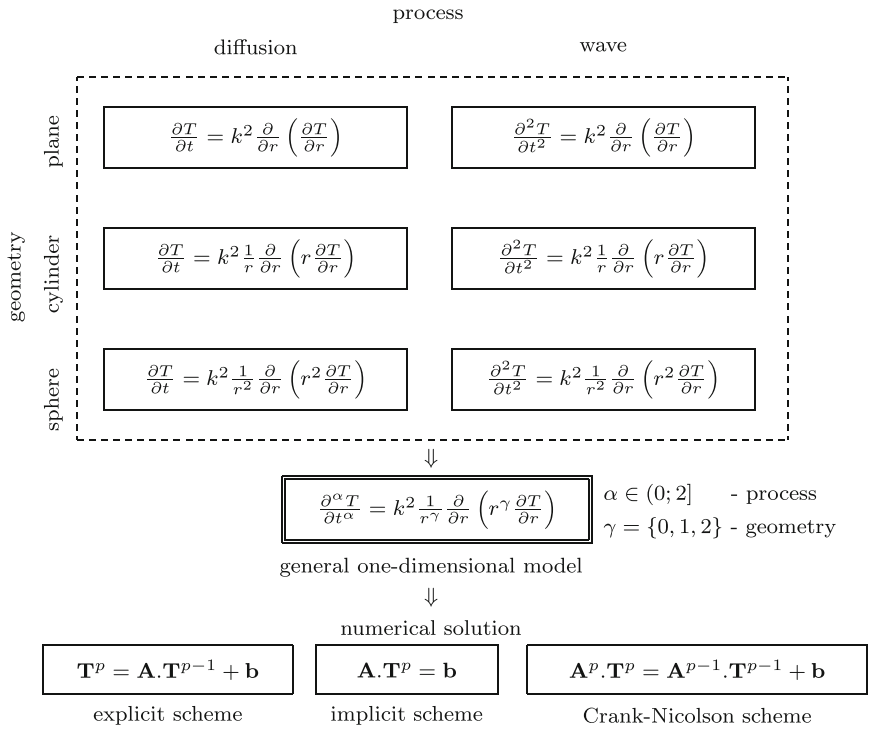

Fig. 1 Graphical abstract of the present paper

– in a long cylinder

$$\varrho c_p \frac{\partial^\alpha T(r,t)}{\partial t^\alpha} = \frac{1}{r}\frac{\partial}{\partial r}\left(r\lambda\frac{\partial T(r,t)}{\partial r}\right),$$

– and in a sphere

$$\varrho c_p \frac{\partial^\alpha T(r,t)}{\partial t^\alpha} = \frac{1}{r^2}\frac{\partial}{\partial r}\left(r^2\lambda\frac{\partial T(r,t)}{\partial r}\right).$$

The examination of the one-dimensional time-fractional heat conduction model in large plane wall, long cylinder, and sphere reveals, that all three equations can be expressed in a compact form as a general model

$$\varrho c_p \frac{\partial^\alpha T(r,t)}{\partial t^\alpha} = \frac{1}{r^\gamma}\frac{\partial}{\partial r}\left(r^\gamma\lambda\frac{\partial T(r,t)}{\partial r}\right). \tag{2.1}$$

In the case of a constant value of the thermal conductivity λ, the general model has the form

$$\frac{\partial^\alpha T(r,t)}{\partial t^\alpha} = k^2\frac{1}{r^\gamma}\frac{\partial}{\partial r}\left(r^\gamma\frac{\partial T(r,t)}{\partial r}\right), \tag{2.2}$$

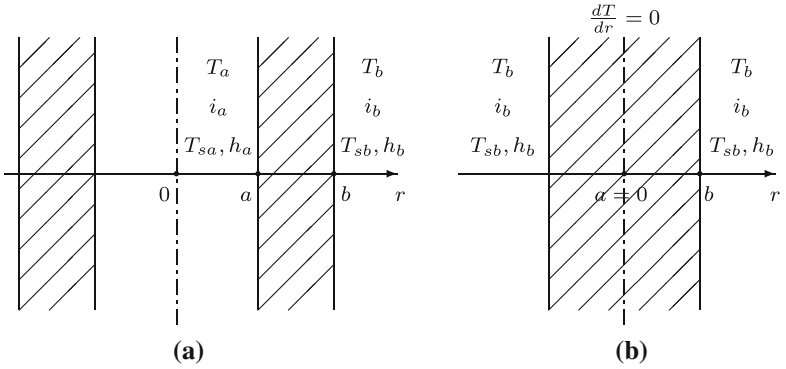

Fig. 2 Boundary conditions for (a) hollow body and (b) full symmetrical body

where γ is a geometric factor (large plane wall $\gamma = 0$, long cylinder $\gamma = 1$, sphere $\gamma = 2$), $k^2 = \lambda/(\varrho c_p)$ is the thermal diffusivity, ϱ is density, and c_p is specific heat capacity.

3 Initial and boundary conditions

The general time-fractional heat conduction model (2.2) requires two boundary conditions, as well as one initial condition. The initial condition specifies the temperature distribution in the material at the begin of the time, that is,

$$T(r, 0) = f_0(r).$$

The boundary conditions specify the temperature or the heat flux at the boundaries of the region. The following boundary conditions (Fig. 2) are considered:

1. *Dirichlet boundary conditions*

$$T(r, t)|_{r=a} = T_a \quad \text{and} \quad T(r, t)|_{r=b} = T_b,$$

where T_a, T_b are temperatures (K) at the boundary surface.

2. *Neumann boundary conditions*

$$-\lambda(r)\frac{\partial T(r, t)}{\partial r}\bigg|_{r=a} = i_a \quad \text{and} \quad -\lambda(r)\frac{\partial T(r, t)}{\partial r}\bigg|_{r=b} = i_b$$

in the special case, i.e. thermal symmetry or full body (Fig. 2b)

$$\frac{\partial T(r, t)}{\partial r}\bigg|_{r=0} = 0,$$

where i_a, i_b stand for heat flux ($\mathrm{W \cdot m^{-2}}$) at the boundary surface.

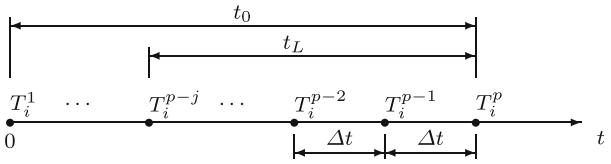

Fig. 3 Time discretisation

3. *Robin boundary conditions*

$$-\lambda(r)\left.\frac{\partial T(r,t)}{\partial r}\right|_{r=a} = h_a\left(T|_{r=a} - T_{sa}\right)$$

and

$$-\lambda(r)\left.\frac{\partial T(r,t)}{\partial r}\right|_{r=b} = h_b\left(T|_{r=b} - T_{sb}\right),$$

where h_a, h_b are heat transfer coefficients ($\mathrm{W{\cdot}m^{-2}{\cdot}K^{-1}}$); T_{sa}, T_{sb} are the surrounding medium temperatures (K) at the boundary surface.

4 Numerical solution

The fractional derivative according to time in the general time-fractional heat conduction model (2.2) is discretised by the backward Euler method and the Grünwald-Letnikov definition

$$\left.\frac{\partial^\alpha T(r,t)}{\partial t^\alpha}\right|_{t_p} \cong \frac{\sum_{j=0}^{N_f} c_j T_i^{p-j}}{\Delta t^\alpha} = \frac{T_i^p + \sum_{j=1}^{N_f} c_j T_i^{p-j}}{\Delta t^\alpha}$$

by using the principle of "*short memory*" (Fig. 3) [26], where t_L is the memory length, Δt is the time step and the value of N_f shall be determined by the following relation

$$N_f = \min\left\{\left[\frac{t_0}{\Delta t}\right], \left[\frac{t_L}{\Delta t}\right]\right\}.$$

For the calculation of the binomial coefficients c_j the following relation can be used

$$c_0 = 1,\ c_j = \left(1 - \frac{1+\alpha}{j}\right) c_{j-1},\ \text{for}\ \ j \geq 1.$$

The derivative according to the spatial coordinate (Fig. 4) is discretised as follows

$$\left.\frac{\partial T(r,t)}{\partial r}\right|_{r_{i-\frac{1}{2}}} \cong \frac{T_i^p - T_{i-1}^p}{\Delta r}$$

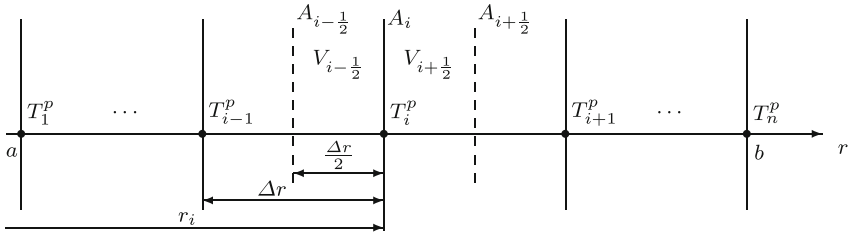

Fig. 4 Space discretisation

$$\left.\frac{\partial T(r,t)}{\partial r}\right|_{r_{i+\frac{1}{2}}} \cong \frac{T_{i+1}^p - T_i^p}{\Delta r}$$

$$\left.\frac{1}{r^\gamma}\frac{\partial}{\partial r}\left(r^\gamma k^2 \frac{\partial T(r,t)}{\partial r}\right)\right|_{r_i} \cong \frac{1}{r_i^\gamma}\frac{r_{i+\frac{1}{2}}^\gamma k_i^2 \left.\frac{\partial T(r,t)}{\partial r}\right|_{r_{i+\frac{1}{2}}} - r_{i-\frac{1}{2}}^\gamma k_{i-1}^2 \left.\frac{\partial T(r,t)}{\partial r}\right|_{r_{i-\frac{1}{2}}}}{\Delta r}$$

$$= \frac{k_i^2 \xi_i T_{i+1}^p - \left(k_i^2 \xi_i + k_{i-1}^2 \zeta_i\right) T_i^p + k_{i-1}^2 \zeta_i T_{i-1}^p}{\Delta r^2},$$

where

$$\xi_i = \left(1 + \frac{\Delta r}{2r_i}\right)^\gamma \quad \text{and} \quad \zeta_i = \left(1 - \frac{\Delta r}{2r_i}\right)^\gamma.$$

The values ξ_i or ζ_i represent the coefficients for calculation of the area $A_{i+\frac{1}{2}}$ or $A_{i-\frac{1}{2}}$ for the selected geometry as follows

$$A_{i+\frac{1}{2}} = A_i \xi_i \quad \text{and} \quad A_{i-\frac{1}{2}} = A_i \zeta_i.$$

Similarly, we can express the relation between area and volume as

$$V_{i+\frac{1}{2}} = A_i \frac{\Delta r}{2}\frac{1}{\mu_i} \quad \text{and} \quad V_{i-\frac{1}{2}} = A_i \frac{\Delta r}{2}\frac{1}{\nu_i},$$

where

$$\mu_i = \frac{(\gamma+1)\frac{\Delta r}{2r_i}}{\left(1 + \frac{\Delta r}{2r_i}\right)^{\gamma+1} - 1} \quad \text{and} \quad \nu_i = \frac{(\gamma+1)\frac{\Delta r}{2r_i}}{1 - \left(1 - \frac{\Delta r}{2r_i}\right)^{\gamma+1}}.$$

4.1 Steady-state

The general time-fractional heat conduction model (2.1) for inhomogeneous material and under steady-state conditions ($\partial T/\partial t = 0$) takes the form

$$\left.\frac{1}{r^\gamma}\frac{\partial}{\partial r}\left(r^\gamma \lambda \frac{\partial T(r,t)}{\partial r}\right)\right|_{r_i} = 0,$$

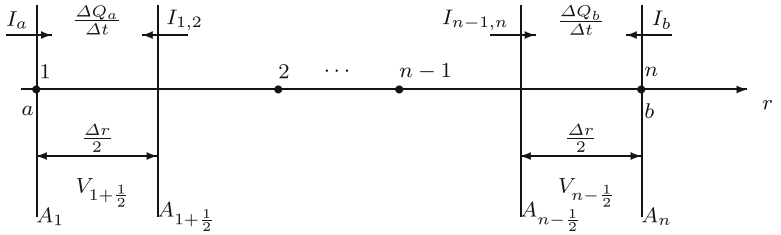

Fig. 5 Scheme for the formulation of boundary conditions

$$\frac{1}{r_i^{\gamma}} \frac{r_{i+\frac{1}{2}}^{\gamma} \lambda_i \frac{\partial T(r,\tau)}{\partial r}\Big|_{r_{i+\frac{1}{2}}} - r_{i-\frac{1}{2}}^{\gamma} \lambda_{i-1} \frac{\partial T(r,\tau)}{\partial r}\Big|_{r_{i-\frac{1}{2}}}}{\Delta r} = 0,$$

$$\lambda_{i-1}\zeta_i T_{i-1} - (\lambda_{i-1}\zeta_i + \lambda_i \xi_i)\, T_i + \lambda_i \xi_i T_{i+1} = 0,$$

and the matrix form is as follows

$$\mathbf{A} \cdot \mathbf{T} = \mathbf{b}$$

or

$$\begin{bmatrix} y_1 & z_1 & 0 & 0 & 0 & 0 \\ x_2 & y_2 & z_2 & 0 & 0 & 0 \\ 0 & x_3 & y_3 & z_3 & 0 & 0 \\ 0 & 0 & \ddots & \ddots & \ddots & 0 \\ 0 & 0 & 0 & x_{n-1} & y_{n-1} & z_{n-1} \\ 0 & 0 & 0 & 0 & x_n & y_n \end{bmatrix} \cdot \begin{bmatrix} T_1 \\ T_2 \\ T_3 \\ \vdots \\ T_{n-1} \\ T_n \end{bmatrix} = \begin{bmatrix} w_1 \\ w_2 \\ w_3 \\ \vdots \\ w_{n-1} \\ w_n \end{bmatrix},$$

where the coefficients are

$$\begin{aligned} x_i &= \lambda_{i-1}\zeta_i, \\ y_i &= -(\lambda_{i-1}\zeta_i + \lambda_i \xi_i), \\ z_i &= \lambda_i \xi_i, \\ w_i &= 0, \quad \text{for} \quad i = 2, 3, \ldots, n-1. \end{aligned}$$

The specified temperatures of the boundary conditions are incorporated by simple assigning the given surface temperatures to the boundary nodes and therefore for the Dirichlet boundary conditions the coefficients are

$$\begin{aligned} y_1 = 1, \quad z_1 = 0, \quad w_1 = T_a, \\ y_n = 1, \quad x_n = 0, \quad w_n = T_b. \end{aligned}$$

When other boundary conditions such as the heat flux or convection are specified at the boundary, the finite difference equation for the node at that boundary is obtained by writing an energy balance of the elementary volume at that boundary (Fig. 5). The energy balance is expressed as

$$0 = I_{1,2} + I_a$$

or

$$0 = A_{1+\frac{1}{2}} \frac{\lambda_1}{\Delta r} (T_2 - T_1) + A_1 i_a,$$

and therefore

$$\xi_1 T_1 - \xi_1 T_2 = R_a i_a.$$

For the Neumann boundary conditions the coefficients are

$$y_1 = \xi_1, \quad z_1 = -\xi_1, \quad w_1 = R_a i_a,$$
$$y_n = \zeta_n, \quad x_n = -\zeta_n, \quad w_n = R_b i_b,$$

where R_a, R_b are internal thermal resistances ($\mathrm{m}^2 \cdot \mathrm{K} \cdot \mathrm{W}^{-1}$).

In the case of Robin boundary conditions the energy balance is expressed as

$$0 = A_{1+\frac{1}{2}} \frac{\lambda_1}{\Delta r} (T_2 - T_1) + A_1 h_a (T_{sa} - T_1)$$

or

$$(\xi_1 + \beta_a) T_1 - \xi_1 T_2 = \beta_a T_{sa}.$$

For the Robin boundary conditions the coefficients are

$$y_1 = \xi_1 + \beta_a, \quad z_1 = -\xi_1, \quad w_1 = \beta_a T_{sa},$$
$$y_n = \zeta_n + \beta_b, \quad x_n = -\zeta_n, \quad w_n = \beta_b T_{sb},$$

where β_a, β_b are Biot numbers or ratios of internal and external thermal resistances at the boundary surface.

4.2 Unsteady-state

According to the type of differential expression finite difference methods can be divided into explicit, implicit and Crank-Nicolson schemes.

4.2.1 Explicit scheme

The explicit scheme for the general time-fractional heat conduction model (2.2) has the form

$$\frac{T_i^p + \sum_{j=1}^{N_f} c_j T_i^{p-j}}{\Delta t^\alpha} = \frac{k_i^2 \xi_i T_{i+1}^{p-1} - (k_i^2 \xi_i + k_{i-1}^2 \zeta_i) T_i^{p-1} + k_{i-1}^2 \zeta_i T_{i-1}^{p-1}}{\Delta r^2}$$

or

$$T_i^p = \tau_{i-1} \zeta_i T_{i-1}^{p-1} - (\tau_{i-1} \zeta_i + \tau_i \xi_i) T_i^{p-1} + \tau_i \xi_i T_{i+1}^{p-1} - \sum_{j=1}^{N_f} c_j T_i^{p-j}, \qquad (4.1)$$

where module τ_i is determined by the relation

$$\tau_i = \left(\frac{k_i}{\Delta r}\right)^2 \Delta t^{\alpha},$$

while the value of τ_i with respect to the stability of the solution must have values less or equal to 0.5.

The matrix form of equation (4.1) is as follows

$$\mathbf{T}^p = \mathbf{A} \cdot \mathbf{T}^{p-1} + \mathbf{b}$$

or

$$\begin{bmatrix} T_1^p \\ T_2^p \\ T_3^p \\ \vdots \\ T_{n-1}^p \\ T_n^p \end{bmatrix} = \begin{bmatrix} y_1 & z_1 & 0 & 0 & 0 & 0 \\ x_2 & y_2 & z_2 & 0 & 0 & 0 \\ 0 & x_3 & y_3 & z_3 & 0 & 0 \\ 0 & 0 & \ddots & \ddots & \ddots & 0 \\ 0 & 0 & 0 & x_{n-1} & y_{n-1} & z_{n-1} \\ 0 & 0 & 0 & 0 & x_n & y_n \end{bmatrix} \cdot \begin{bmatrix} T_1^{p-1} \\ T_2^{p-1} \\ T_3^{p-1} \\ \vdots \\ T_{n-1}^{p-1} \\ T_n^{p-1} \end{bmatrix} + \begin{bmatrix} w_1 \\ w_2 \\ w_3 \\ \vdots \\ w_{n-1} \\ w_n \end{bmatrix},$$

where the coefficients are

$$\begin{aligned} x_i &= \tau_{i-1}\zeta_i, \\ y_i &= -\left(\tau_{i-1}\zeta_i + \tau_i\xi_i\right), \\ z_i &= \tau_i\xi_i, \\ w_i &= -\sum_{j=1}^{N_f} c_j T_i^{p-j}, \quad \text{for} \quad i = 2, 3, \ldots, n-1. \end{aligned}$$

For the Dirichlet boundary conditions the coefficients are

$$\begin{aligned} y_1 = 0, \quad z_1 = 0, \quad w_1 = T_a, \\ y_n = 0, \quad x_n = 0, \quad w_n = T_b. \end{aligned}$$

In the case of Neumann boundary conditions the energy balance is expressed as

$$\frac{\Delta Q_a}{\Delta t} = I_{1,2} + I_a$$

or

$$\varrho_1 c_{p1} V_{1+\frac{1}{2}} \frac{T_1^p + \sum_{j=1}^{N_f} c_j T_1^{p-j}}{\Delta t} = A_{1+\frac{1}{2}} \frac{\lambda_1}{\Delta r}\left(T_2^{p-1} - T_1^{p-1}\right) + A_1 i_a,$$

and therefore

$$T_1^p = -2\tau_1\mu_1\xi_1 T_1^{p-1} + 2\tau_1\mu_1\xi_1 T_2^{p-1} - \sum_{j=1}^{N_f} c_j T_1^{p-j} + 2\tau_1\mu_1 R_a i_a.$$

For the Neumann boundary conditions the coefficients are

$$\begin{aligned} y_1 &= -2\tau_1\mu_1\xi_1, \quad z_1 = 2\tau_1\mu_1\xi_1, \\ w_1 &= -\sum_{j=1}^{N_f} c_j T_1^{p-j} + 2\tau_1\mu_1 R_a i_a, \\ y_n &= -2\tau_{n-1}\nu_n\zeta_n, \quad x_n = 2\tau_{n-1}\nu_n\zeta_n, \\ w_n &= -\sum_{j=1}^{N_f} c_j T_n^{p-j} + 2\tau_{n-1}\nu_n R_b i_b. \end{aligned}$$

In the case of Robin boundary conditions the energy balance is expressed as

$$\varrho_1 c_{p1} V_{1+\frac{1}{2}} \frac{T_1^p + \sum_{j=1}^{N_f} c_j T_1^{p-j}}{\Delta t} = A_{1+\frac{1}{2}} \frac{\lambda_1}{\Delta r} \left(T_2^{p-1} - T_1^{p-1}\right) + A_1 h_a \left(T_{sa} - T_1^{p-1}\right)$$

or

$$T_1^p = -2\tau_1\mu_1 \left(\xi_1 + \beta_a\right) T_1^{p-1} + 2\tau_1\mu_1\xi_1 T_2^{p-1} - \sum_{j=1}^{N_f} c_j T_1^{p-j} + 2\tau_1\mu_1\beta_a T_{sa}.$$

For the Robin boundary conditions the coefficients are

$$\begin{aligned} y_1 &= -2\tau_1\mu_1 \left(\xi_1 + \beta_a\right), \quad z_1 = 2\tau_1\mu_1\xi_1, \\ w_1 &= -\sum_{j=1}^{N_f} c_j T_1^{p-j} + 2\tau_1\mu_1\beta_a T_{sa}, \\ y_n &= -2\tau_{n-1}\nu_n \left(\zeta_n + \beta_b\right), \quad x_n = 2\tau_{n-1}\nu_n\zeta_n, \\ w_n &= -\sum_{j=1}^{N_f} c_j T_n^{p-j} + 2\tau_{n-1}\nu_n\beta_b T_{sb}, \end{aligned}$$

where R_a, R_b are internal thermal resistances ($\mathrm{m}^2\cdot\mathrm{K}\cdot\mathrm{W}^{-1}$); β_a, β_b are Biot numbers or ratios of internal and external thermal resistances at the boundary surface.

4.2.2 Implicit scheme

The implicit scheme for the general time-fractional heat conduction model (2.2) has the form

$$\frac{T_i^p + \sum_{j=1}^{N_f} c_j T_i^{p-j}}{\Delta t^\alpha} = \frac{k_i^2\xi_i T_{i+1}^p - (k_i^2\xi_i + k_{i-1}^2\zeta_i) T_i^p + k_{i-1}^2\zeta_i T_{i-1}^p}{\Delta r^2},$$

or

$$-\tau_{i-1}\zeta_i T_{i-1}^p + (1 + \tau_{i-1}\zeta_i + \tau_i\xi_i)\, T_i^p - \tau_i\xi_i T_{i+1}^p = -\sum_{j=1}^{N_f} c_j T_i^{p-j}.$$

In matrix form this is

$$\mathbf{A}\cdot\mathbf{T}^p = \mathbf{b}$$

or

$$\begin{bmatrix} y_1 & z_1 & 0 & 0 & 0 & 0 \\ x_2 & y_2 & z_2 & 0 & 0 & 0 \\ 0 & x_3 & y_3 & z_3 & 0 & 0 \\ 0 & 0 & \ddots & \ddots & \ddots & 0 \\ 0 & 0 & 0 & x_{n-1} & y_{n-1} & z_{n-1} \\ 0 & 0 & 0 & 0 & x_n & y_n \end{bmatrix} \cdot \begin{bmatrix} T_1^p \\ T_2^p \\ T_3^p \\ \vdots \\ T_{n-1}^p \\ T_n^p \end{bmatrix} = \begin{bmatrix} w_1 \\ w_2 \\ w_3 \\ \vdots \\ w_{n-1} \\ w_n \end{bmatrix},$$

where the coefficients are

$$\begin{aligned} x_i &= -\tau_{i-1}\zeta_i, \\ y_i &= 1 + \tau_{i-1}\zeta_i + \tau_i\xi_i, \\ z_i &= -\tau_i\xi_i, \\ w_i &= -\sum_{j=1}^{N_f} c_j T_i^{p-j}, \quad \text{for} \quad i = 2, 3, \ldots, n-1. \end{aligned}$$

For the Dirichlet boundary conditions the coefficients are

$$\begin{aligned} y_1 = 1, \quad z_1 = 0, \quad w_1 = T_a, \\ y_n = 1, \quad x_n = 0, \quad w_n = T_b. \end{aligned}$$

For the Neumann boundary conditions the coefficients are

$$\begin{aligned} y_1 &= 1 + 2\tau_1\mu_1\xi_1, \quad z_1 = -2\tau_1\mu_1\xi_1, \\ w_1 &= -\sum_{j=1}^{N_f} c_j T_1^{p-j} + 2\tau_1\mu_1 R_a i_a, \\ y_n &= 1 + 2\tau_{n-1}\nu_n\zeta_n, \quad x_n = -2\tau_{n-1}\nu_n\zeta_n, \\ w_n &= -\sum_{j=1}^{N_f} c_j T_n^{p-j} + 2\tau_{n-1}\nu_n R_b i_b. \end{aligned}$$

For the Robin boundary conditions the coefficients are

$$y_1 = 1 + 2\tau_1\mu_1\left(\xi_1 + \beta_a\right), \quad z_1 = -2\tau_1\mu_1\xi_1,$$

$$
\begin{aligned}
w_1 &= -\sum_{j=1}^{N_f} c_j T_1^{p-j} + 2\tau_1 \mu_1 \beta_a T_{sa}, \\
y_n &= 1 + 2\tau_{n-1} \nu_n \left(\zeta_n + \beta_b\right), \quad x_n = -2\tau_{n-1} \nu_n \zeta_n, \\
w_n &= -\sum_{j=1}^{N_f} c_j T_n^{p-j} + 2\tau_{n-1} \nu_n \beta_b T_{sb}.
\end{aligned}
$$

4.2.3 Crank-Nicolson scheme

The Crank-Nicolson scheme for the general time-fractional heat conduction model (2.2) has the form

$$
\begin{aligned}
\frac{T_i^p + \sum_{j=1}^{N_f} c_j T_i^{p-j}}{\Delta t^\alpha} &= \frac{1}{2}\left(\frac{k_i^2 \xi_i T_{i+1}^{p-1} - (k_i^2 \xi_i + k_{i-1}^2 \zeta_i) T_i^{p-1} + k_{i-1}^2 \zeta_i T_{i-1}^{p-1}}{\Delta r^2}\right) \\
&\quad + \frac{1}{2}\left(\frac{k_i^2 \xi_i T_{i+1}^{p} - (k_i^2 \xi_i + k_{i-1}^2 \zeta_i) T_i^{p} + k_{i-1}^2 \zeta_i T_{i-1}^{p}}{\Delta r^2}\right)
\end{aligned}
$$

or

$$
\begin{aligned}
&- \tau_{i-1}\zeta_i T_{i-1}^p + \left(2 + \tau_{i-1}\zeta_i + \tau_i \xi_i\right) T_i^p - \tau_i \xi_i T_{i+1}^p \\
&= \tau_{i-1}\zeta_i T_{i-1}^{p-1} - \left(\tau_{i-1}\zeta_i + \tau_i \xi_i\right) T_i^{p-1} + \tau_i \xi_i T_{i+1}^{p-1} - 2\sum_{j=1}^{N_f} c_j T_i^{p-j}.
\end{aligned}
$$

In matrix form this is

$$
\mathbf{A}^p \cdot \mathbf{T}^p = \mathbf{A}^{p-1} \cdot \mathbf{T}^{p-1} + \mathbf{b}
$$

or

$$
\begin{bmatrix}
y_1 & z_1 & 0 & 0 & 0 & 0 \\
x_2 & y_2 & z_2 & 0 & 0 & 0 \\
0 & x_3 & y_3 & z_3 & 0 & 0 \\
0 & 0 & \ddots & \ddots & \ddots & 0 \\
0 & 0 & 0 & x_{n-1} & y_{n-1} & z_{n-1} \\
0 & 0 & 0 & 0 & x_n & y_n
\end{bmatrix}
\cdot
\begin{bmatrix}
T_1^p \\ T_2^p \\ T_3^p \\ \vdots \\ T_{n-1}^p \\ T_n^p
\end{bmatrix} =
$$

$$
\begin{bmatrix}
0 & 0 & 0 & 0 & 0 & 0 \\
-x_2 & 2 - y_2 & -z_2 & 0 & 0 & 0 \\
0 & -x_3 & 2 - y_3 & -z_3 & 0 & 0 \\
0 & 0 & \ddots & \ddots & \ddots & 0 \\
0 & 0 & 0 & -x_{n-1} & 2 - y_{n-1} & -z_{n-1} \\
0 & 0 & 0 & 0 & 0 & 0
\end{bmatrix}
\cdot
\begin{bmatrix}
T_1^{p-1} \\ T_2^{p-1} \\ T_3^{p-1} \\ \vdots \\ T_{n-1}^{p-1} \\ T_n^{p-1}
\end{bmatrix} +
\begin{bmatrix}
w_1 \\ w_2 \\ w_3 \\ \vdots \\ w_{n-1} \\ w_n
\end{bmatrix},
$$

where the coefficients are

$$\begin{aligned} x_i &= -\tau_{i-1}\zeta_i, \\ z_i &= -\tau_i\xi_i, \\ y_i &= 2 + \tau_{i-1}\zeta_i + \tau_i\xi_i, \\ w_i &= -2\sum_{j=1}^{N_f} c_j T_i^{p-j}, \quad \text{for} \quad i = 2, 3, \ldots, n-1. \end{aligned}$$

For the Dirichlet boundary conditions the coefficients are

$$\begin{aligned} y_1 = 1, \quad z_1 = 0, \quad w_1 = T_a, \\ y_n = 1, \quad x_n = 0, \quad w_n = T_b. \end{aligned}$$

For the Neumann boundary conditions the coefficients are

$$\begin{aligned} y_1 &= 1 + 2\tau_1\mu_1\xi_1, \quad z_1 = -2\tau_1\mu_1\xi_1, \\ w_1 &= -\sum_{j=1}^{N_f} c_j T_1^{p-j} + 2\tau_1\mu_1 R_a i_a, \\ y_n &= 1 + 2\tau_{n-1}\nu_n\zeta_n, \quad x_n = -2\tau_{n-1}\nu_n\zeta_n, \\ w_n &= -\sum_{j=1}^{N_f} c_j T_n^{p-j} + 2\tau_{n-1}\nu_n R_b i_b. \end{aligned}$$

For the Robin boundary conditions the coefficients are

$$\begin{aligned} y_1 &= 1 + 2\tau_1\mu_1\left(\xi_1 + \beta_a\right), \quad z_1 = -2\tau_1\mu_1\xi_1, \\ w_1 &= -\sum_{j=1}^{N_f} c_j T_1^{p-j} + 2\tau_1\mu_1\beta_a T_{sa}, \\ y_n &= 1 + 2\tau_{n-1}\nu_n\left(\zeta_n + \beta_b\right), \quad x_n = -2\tau_{n-1}\nu_n\zeta_n, \\ w_n &= -\sum_{j=1}^{N_f} c_j T_n^{p-j} + 2\tau_{n-1}\nu_n\beta_b T_{sb}. \end{aligned}$$

5 Implementation

The implementation was realised in the programming environment MATLAB, in which the functions for solution of the time-fractional diffusion-wave equation in various geometries have been created. The MATLAB toolbox called *Time-Fractional Diffusion-Wave Eq. in Various Geometries* (`TFDWEg`) consists of functions for solving one-dimensional general model for various geometries with utilisation of the explicit,

implicit, and Crank-Nicolson scheme, respectively. The functions implement the finite difference method for homogeneous or inhomogeneous material and for homogeneous or inhomogeneous boundary conditions. The functions headers are as follows

```
function [R,T,MU] = TFDWEg_exp(Uin,alpha,Nf,k,dr,a,b,dt,ts,TBC,BC,g)

function [R,T,MU] = TFDWEg_imp(Uin,alpha,Nf,k,dr,a,b,dt,ts,TBC,BC,g)

function [R,T,MU] = TFDWEg_CN (Uin,alpha,Nf,k,dr,a,b,dt,ts,TBC,BC,g)
```

where the function inputs are: `Uin` is the vector of the initial conditions, `alpha` is the order of the time derivative, `Nf` is the memory length, `k` is the process coefficients vector, `dr` is the spatial step, `a` and `b` are the left, right side coordinates of the body, respectively, `dt` is the time step, `ts` is the time of simulation, `TBC` is the vector of the boundary conditions type, `BC` are the values of the boundary condition, and `g` is the geometry type. The function outputs are: `R` is the vector of coordinates, `T` is the vector of time, and `MU` is the output values matrix. The toolbox is published at MathWorks, Inc., MATLAB Central File Exchange [40].

6 Simulations

Time-Fractional Diffusion-Wave Equation simulations in various geometries for homogeneous or inhomogeneous material and for homogeneous or inhomogeneous boundary conditions are realised using the script `TFDWEg_test.m` which is a part of the toolbox `TFDWEg` [40]. In the following examples the behaviour of temperature in space and time for various geometries is illustrated.

Let us propose an example, where the initial conditions are been defined in the form of the constant temperature ($T(r, 0) = 0°\text{C}$) in the whole cross-section, considering copper as the material (with density $\varrho = 8900$ kg/m^3, thermal conductivity $\lambda = 400$ W/m/K, specific heat capacity $c_p = 380$ J/kg/K), left ($a = 0.01$ m) and right ($b = 0.03$ m) side coordinate. The material was divided into twenty parts in the space, with time step (0.001 s), total time simulation (2 s), and Dirichlet boundary conditions with temperatures at the edges ($T_a = 0°\text{C}$ and $T_b = 15°\text{C}$). The simulation results using Crank-Nicolson scheme are shown in Fig. 6, where the left coloumn shows the behaviour of temperature in time (where the parameter is the position in space), the middle coloumn shows the behaviour of temperature in space (where the parameter is time), and the right coloumn displays 3D plots of temperatures in space and time for hollow body (Fig. 2a), i.e. large plane wall (Fig. 6a), long cylinder (Fig. 6b), and sphere (Fig. 6c). In the case of setting the left coordinate to zero ($a = 0.0$ m), it is possible to perform the same simulation but for a full symmetrical body (Fig. 2b), as shown in figure Fig. 7.

The graphs in Fig. 8 show the evolution results solving the time-fractional heat conduction using the fractional-order derivative $\alpha = 0.5$, 1.0, and 1.5, respectively. Comparing the graphs, one can observe that the derivative of order 0.5 exhibits fast temperature rise in the beginning and slow temperature rise later. Moreover, it is evident that the temperatures propagate and diffuse with time, which means that the

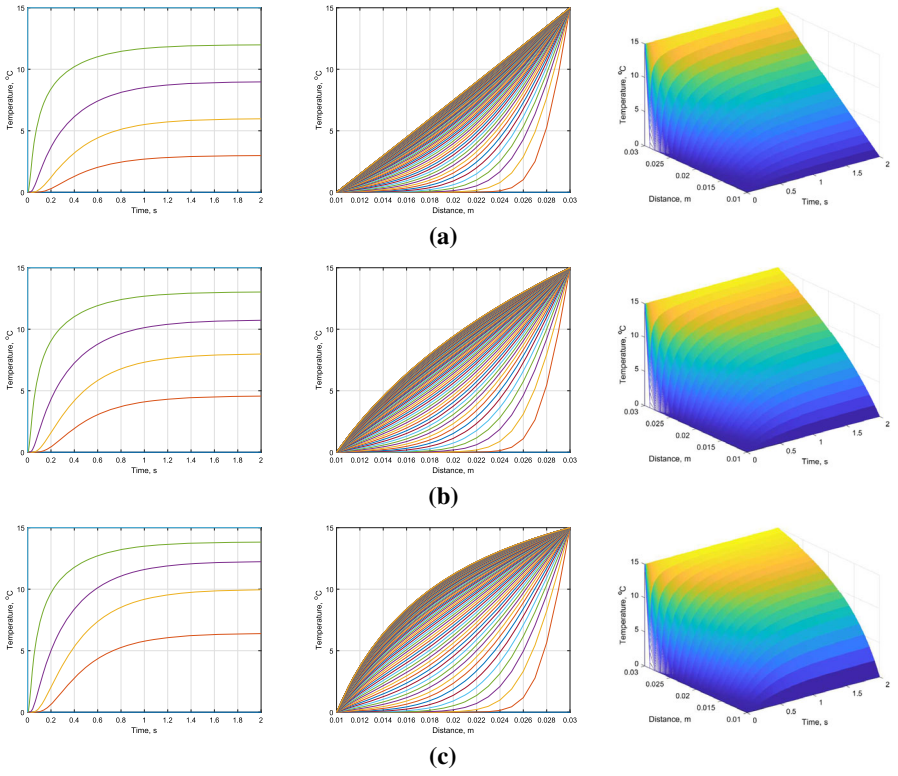

Fig. 6 Hollow body – (a) large plane wall, (b) long cylinder, and (c) sphere

temperature continuously depends on the fractional derivative, therefore, when $\alpha = 1.5$, both diffusion and wave response can be observed.

Let us use the previous settings to perform simulations demonstrating the use of different homogeneous boundary conditions for homogeneous material. The behaviour of the temperature for the Dirichlet, Neumann, and Robin boundary conditions is shown in Fig. 9. In the case of the Dirichlet boundary conditions, the surface temperatures are $T_a = T_b = 15°\text{C}$; in the case of the Neumann boundary conditions, the thermal flux and the internal thermal resistance are $i_a \cdot R_a = i_b \cdot R_b = 0.75°\text{C}$, and in the case of the Robin boundary conditions the surrounding media temperatures and the ratio of internal and external thermal resistances are $T_{sa} = T_{sb} = 15°\text{C}$, $\beta_a = \beta_b = 1$. The graphs in Fig. 10 show inhomogeneous boundary conditions for selected combinations, i.e. Neumann-Dirichlet, Robin-Dirichlet, and Neumann-Robin, respectively.

The script `TFDWEg_test.m` also allows to simulate homogeneous as well as inhomogeneous material. For example, in the case of thermal diffusivity for twenty layers and two materials (brass and copper) of the same thickness a twenty-component thermal diffusivity vector is needed (ten components for brass and ten components for copper). Results of the simulations are shown in Fig. 11a for homogeneous and in Fig. 11b for inhomogeneous material, where in the first half of the specimen length there is a lower

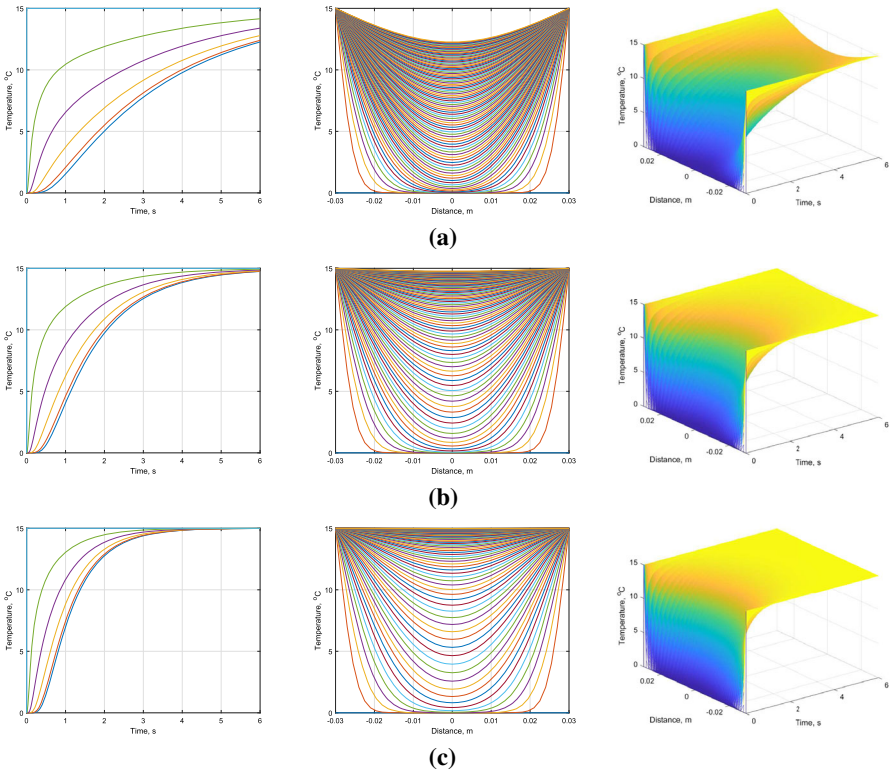

Fig. 7 Symmetrical body – (a) large plane wall, (b) long cylinder, and (c) sphere

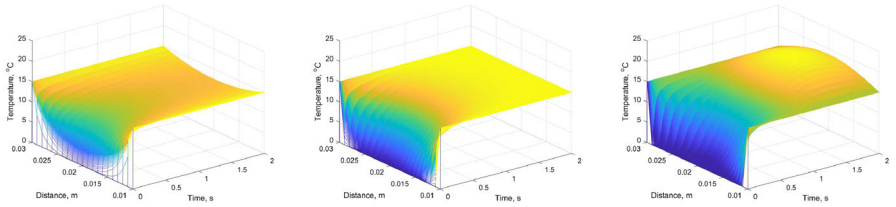

Fig. 8 Large plane wall for α=0.5, 1.0, and 1.5

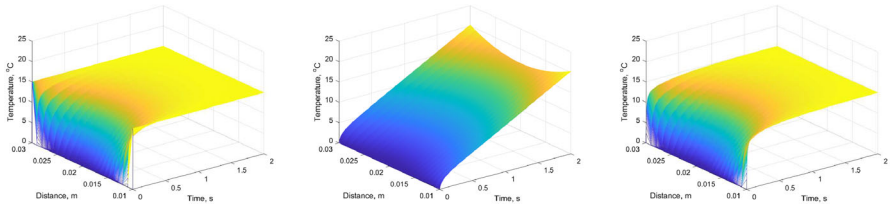

Fig. 9 Dirichlet, Neumann, and Robin homogeneous boundary conditions for large plane wall

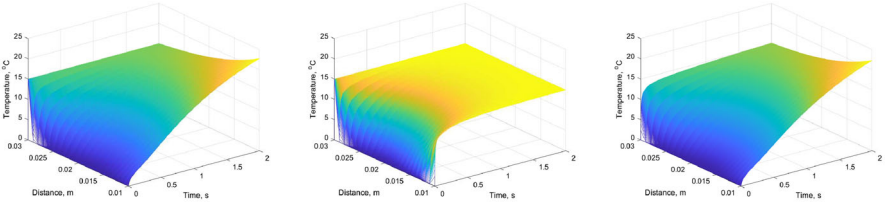

Fig. 10 Neumann-Dirichlet, Robin-Dirichlet, and Neumann-Robin inhomogeneous boundary conditions

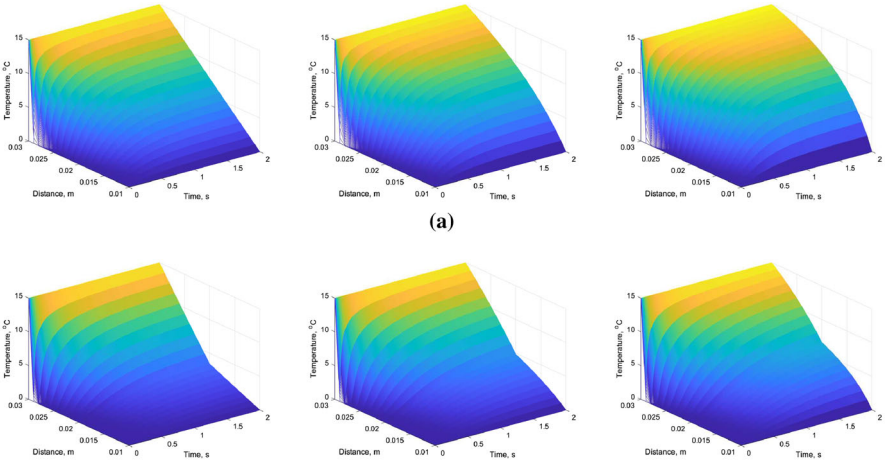

Fig. 11 Large plane wall, long cylinder, and sphere for (a) homogeneous and (b) inhomogeneous material

temperature rise than in the other half. This is due to the fact that in the first half the material there is copper whose thermal diffusivity is about three times larger than that of brass.

7 Conclusion

The general one-dimensional model of the time-fractional diffusion-wave equation in various geometries is designed and described in this contribution. The numerical solution using the Grünwald-Letnikov definition of fractional derivative according to time for homogeneous and inhomogeneous boundary conditions and for homogeneous and inhomogeneous material is presented. The numerical schemes were implemented in MATLAB in the form of a library of functions. The possibilities of using this library are illustrated by examples and simulations. Additionally, besides modeling heat conduction processes, the library allows to model other processes such as diffusion, wave distribution, and so on. The library is a suitable tool for the implementation of simulations of a wide class of processes and also for the creation of complex models in the MATLAB environment. Benefits of this work are the design, numerical solution

and implementation of one general mathematical model that can be used for modeling various different processes, in various geometries, materials and boundary conditions.

Acknowledgements This work was supported by the Slovak Research and Development Agency under the contract No. APVV-14-0892, APVV-18-0526, SK-SRB-21-0028, and by project VEGA 1/0674/23.

Declarations

Conflict of interest The authors declare that they have no conflict of interest.

References

1. Abouelregal, A.E.: Thermoelastic Interaction in an Infinite Long Hollow Cylinder with Fractional Heat Conduction Equation. Advances in Applied Mathematics and Mechanics **9**(2), 378–392 (2017). https://doi.org/10.4208/aamm.2015.m26
2. Agrawal, O.P.: A numerical scheme for initial compliance and creep response of a system. Mechanics Research Communications **36**(4), 444–451 (2009). https://doi.org/10.1016/j.mechrescom.2008.12.010
3. Chua, Lo., Pivka, L., Wu, Cw.: A universal circuit for studying chaotic phenomena. Philosophical Transactions of the Royal Society of London **353**, 65–84 (1995). https://doi.org/10.1098/rsta.1995.0091
4. Consiglio, A., Mainardi, F.: On the evolution of fractional diffusive wave. Ricerche di Matematica **70**(1), 21–33 (2021). https://doi.org/10.48550/arXiv.1910.12595
5. Ervin, V.J., Roop, J.P.: Variational solution of the fractional advection dispersion equations on bounded domains in $\mathbb{R}^d$. Numerical Methods for Partial Differential Equations **23**(2), 256–281 (2006). https://doi.org/10.1002/num.20169
6. Fix, G.J., Roof, J.P.: Least squares finite-element solution of a fractional order two-point boundary value problem. Computers & Mathematics with Applications **48**(7–8), 1017–1033 (2004). https://doi.org/10.1016/j.camwa.2004.10.003
7. Fulger, D., Scalas, E., Germano, G.: Monte Carlo simulation of uncoupled continuous-time random walks yielding a stochastic solution of the space-time fractional diffusion equation. Physical Review E **77**(2), 1–7 (2008). https://doi.org/10.1103/PhysRevE.77.021122
8. Gorenflo, R., Vivoli, A.: Fully discrete random walks for space-time fractional diffusion equations. Signal Processing **83**(11), 2411–2420 (2003). https://doi.org/10.1016/S0165-1684(03)00193-2
9. Ilic, M., Turner, I.W., Simpson, D.P.: A restarted Lanczos approximation to functions of a symmetric matrix. IMA Journal of Numerical Analysis **30**(4), 1044–1061 (2010). https://doi.org/10.1093/imanum/drp003
10. Jafari, H., Daftardar-Gejji, V.: Solving linear and nonlinear fractional diffusion and wave equations by Adomian decomposition. Applied Mathematics and Computation **180**(2), 488–497 (2006). https://doi.org/10.1016/j.amc.2005.12.031
11. Kukla, S., Siedlecka, U.: Fractional heat conduction in a sphere under mathematical and physical Robin conditions. Journal of Theoretical and Applied Mechanics **56**(2), 339–349 (2018). https://doi.org/10.15632/jtam-pl.56.2.339

12. Kumar, P., Agrawal, O.P.: An approximate method for numerical solution of fractional differential equations. Signal Processing **86**(10), 2602–2610 (2006). https://doi.org/10.1016/j.sigpro.2006.02.007
13. Leszczynski, J.S.: An Introduction to Fractional Mechanics. The Publishing Office of Czestochowa University of Technology, Czestochowa (2011)
14. Liu, F., Shen, S., Anh, V., Turner, I.: Analysis of a discrete non-Markovian random walk approximation for the time fractional diffusion equation. ANZIAM Journal **46**(5), 488–504 (2005). https://doi.org/10.21914/anziamj.v46i0.973
15. Liu, F., Liu, F., Turner, I., Anh, V.: Approximation of the Lévy-Feller advection-dispersion process by random walk and finite difference method. Journal of Computational Physics **222**(1), 57–70 (2007). https://doi.org/10.1016/j.jcp.2006.06.005
16. Mandelbrot, B.: Some Noises with 1/f Spectrum, a Bridge Between Direct Current and White Noise. IEEE Transactions on Information Theory **13**(2), 289–298 (1967). https://doi.org/10.1109/TIT.1967.1053992
17. Marseguerra, M.M., Zoia, A.: Monte Carlo evaluation of FADE approach to anamalous kinetics. Mathematics and Computers in Simulation **77**(4), 345–357 (2008). https://doi.org/10.1016/j.matcom.2007.03.001
18. Minerbo, G.N., Ross, B.: An Introduction to the Fractional Calculus and Fractional Differential Equations. John Wiley & Sons Inc., New York (1993)
19. Momani, S., Odibat, Z.: Numerical solutions of the space-time fractional advection-dispersion equation. Numerical Methods for Partial Differential Equations **24**(6), 1416–1429 (2008). https://doi.org/10.1002/num.20324
20. Mukherjee, A., Lahiri, A., Mishra, S.C.: Analyses of dual-phase lag heat conduction in 1-D cylindrical and spherical geometry - An application of the lattice Boltzmann method. International Journal of Heat and Mass Transfer **96**, 627–642 (2016). https://doi.org/10.1016/j.ijheatmasstransfer.2016.01.048
21. Oldham, K.B.: Semiintegral electroanalysis: Analog implementation. Analytical Chemistry **45**(1), 39–47 (1973). https://doi.org/10.1021/ac60323a005
22. Oldham, K.B., Spanier, J.: The Fractional Calculus. Academic press, New York (1974)
23. Oldham, K.B., Zoski, C.G.: Analogue instrumentation for processing polarographic data. Journal of Electroanalytical Chemistry and Interfacial Electrochemistry **157**, 27–51 (1983). https://doi.org/10.1016/S0022-0728(83)80374-X
24. Petras, I.: Fractional-Order Nonlinear Systems: Modeling. Analysis and Simulation. Higher Education Press, Beijing (2011)
25. Petras, I., Terpak, J.: Fractional Calculus as a Simple Tool for Modeling and Analysis of Long Memory Process in Industry. Mathematics **7**(6), 1–9 (2019). https://doi.org/10.3390/math7060511
26. Podlubny, I.: Fractional Differential Equations. Academic Press, San Diego (1999)
27. Podlubny, I.: Matrix approach to discrete fractional calculus. Fractional Calculus and Applied Analysis **3**(4), 359–386 (2000)
28. Podlubny, I., Chechkin, A., Skovranek, T., Chen, Y.Q., Vinagre, B.J.: Matrix approach to discrete fractional calculus II: Partial fractional differential equations. Journal of Computational Physics **228**, 3137–3153 (2009). https://doi.org/10.1016/j.jcp.2009.01.014
29. Podlubny, I., Skovranek, T., Vinagre, B.J., Petras, I., Chen, Y.Q.: Matrix approach to discrete fractional calculus 3: non-equidistant grids, variable step length and distributed orders. Philosophical Transactions of the Royal Society A **371**(1990), 1–15 (2013). https://doi.org/10.1098/rsta.2012.0153
30. Leonenko, N., Podlubny, I.: Monte Carlo method for fractional-order differentiation extended to higher orders. Fractional Calculus and Applied Analysis **25**(3), 841–857 (2022). https://doi.org/10.1007/s13540-022-00048-w
31. Povstenko, Y.: Time-fractional heat conduction in a two-layer composite slab. Fractional Calculus and Applied Analysis **19**(4), 940–953 (2016). https://doi.org/10.1515/fca-2016-0051
32. Povstenko, Y., Klekot, J.: Fractional heat conduction with heat absorption in a sphere under Dirichlet boundary condition. Computational & Applied Mathematics **37**(4), 4475–4483 (2018). https://doi.org/10.1007/s40314-018-0585-7
33. Roop, J.P.: Computational aspects of FEM approximation of fractional advection dispersion equation on bounded domains in R^2. Journal of Computation and Applied Mathematics **193**(1), 243–268 (2006). https://doi.org/10.1016/j.cam.2005.06.005
34. Ross, B.: An Brief History and Exposition of the Fundamental Theory of the Fractional Calculus. Lecture Notes in Mathematics **457**, 1–36 (1975). https://doi.org/10.1007/BFb0067096

35. Sakakibara, S.: Properties of Vibration with Fractional Derivatives Damping of Order 1/2. JSME International Journal **40**(3), 393–399 (1997). https://doi.org/10.1299/jsmec.40.393
36. Samko, S.G., Kilbas, A.A., Marichev, O.I.: Fractional Integrals and Derivatives and Some of Their Applications. Nauka i Technika, Minsk (1987)
37. Shen, S., Liu, F., Anh, V., Turner, I.: Error analysis of an explicit finite difference approximation for the space fractional diffusion equation with insulated ends. ANZIAM Journal **46**(E), 871–889 (2005). https://doi.org/10.21914/anziamj.v46i0.995
38. Siedlecka, U., Kukla, S.: A Solution to the Problem of Time-Fractional Heat Conduction in a Multi-layer Slab. Journal of Applied Mechanics and Computational Mechanics **14**(3), 95–102 (2015). https://doi.org/10.17512/jamcm.2015.3.10
39. Tadjeran, C., Meerschaert, M.M.: A second-order accurate numerical approximation for the two-dimensional fractional diffusion equation. Journal of Computational Physics **220**(2), 813–823 (2007). https://doi.org/10.1016/j.jcp.2006.05.030
40. Terpak, J.: Time-Fractional Diffusion-Wave Eq. in Various Geometries. MATLAB Central File Exchange (2022). https://www.mathworks.com/matlabcentral/fileexchange/114685-time-fractional-diffusion-wave-eq-in-various-geometries
41. Torvik, P.J., Bagley, R.L.: On the appearance of the fractional derivative in the behavior of real materials. Transactions of the ASME **51**, 294–298 (1984). https://doi.org/10.1115/1.3167615
42. Wang, X.Y., Zhang, X.P., Ma, Ch.: Modified projective synchronization of fractional-order chaotic systems via active sliding mode control. Nonlinear Dynamics **69**(1), 511–517 (2012). https://doi.org/10.1007/s11071-011-0282-1
43. Yuan, L., Agrawal, O.P.: A numerical scheme for dynamic systems containing fractional derivatives. Journal of Vibration and Acoustics **124**(2), 321–324 (2002). https://doi.org/10.1115/1.1448322
44. Zecova, M., Terpak, J.: Heat conduction modeling by using fractional-order derivatives. Applied Mathematics and Computation **257**, 365–373 (2015). https://doi.org/10.1016/j.amc.2014.12.136
45. Zhang, X.Y., Li, X.F.: Transient thermal stress intensity factors for a circumferential crack in a hollow cylinder based on generalized fractional heat conduction. Internationa Journal of Thermal Sciences **121**, 336–347 (2017). https://doi.org/10.1016/j.ijthermalsci.2017.07.015
46. Zhuang, P., Liu, F.: Implicit difference approximation for the time fractional diffusion equation. Journal of Applied Mathematics and Computing **22**(3), 87–99 (2006). https://doi.org/10.1007/BF02832039